

# Different corrosion behaviour of CuNi10Fe1Mn alloy condenser tubes in seawater

---

Dadić, Zvonimir; Gudić, Senka; Vrsalović, Ladislav; Kvirgić, Dario; Ivanić, Ivana; Čatipović, Nikša

Source / Izvornik: **Mechanical Technologies and Structural Materials 2019 Conference proceedings, 2019, 25 - 31**

Conference paper / Rad u zborniku

Publication status / Verzija rada: **Published version / Objavljena verzija rada (izdavačev PDF)**

Permanent link / Trajna poveznica: <https://urn.nsk.hr/urn:nbn:hr:115:977236>

Rights / Prava: [In copyright](#) / [Zaštićeno autorskim pravom.](#)

Download date / Datum preuzimanja: **2025-03-21**



SVEUČILIŠTE U ZAGREBU  
METALURŠKI FAKULTET  
UNIVERSITY OF ZAGREB  
FACULTY OF METALLURGY

Repository / Repozitorij:

[Repository of Faculty of Metallurgy University of Zagreb - Repository of Faculty of Metallurgy University of Zagreb](#)





HRVATSKO DRUŠTVO  
ZA STROJARSKE TEHNOLOGIJE  
CROATIAN SOCIETY  
FOR MECHANICAL TECHNOLOGIES

In association with:



University of Split  
Faculty of Electrical Engineering,  
Mechanical Engineering and  
Naval Architecture



Slovak Academy of Science  
Institute of Materials and  
Machine Mechanics



Sveučilište u Splitu  
Sveučilišni  
odjel za stručne studije



Croatian Society for  
Materials and Tribology



Dublin Institute  
of Technology



Rogante Engineering  
Office

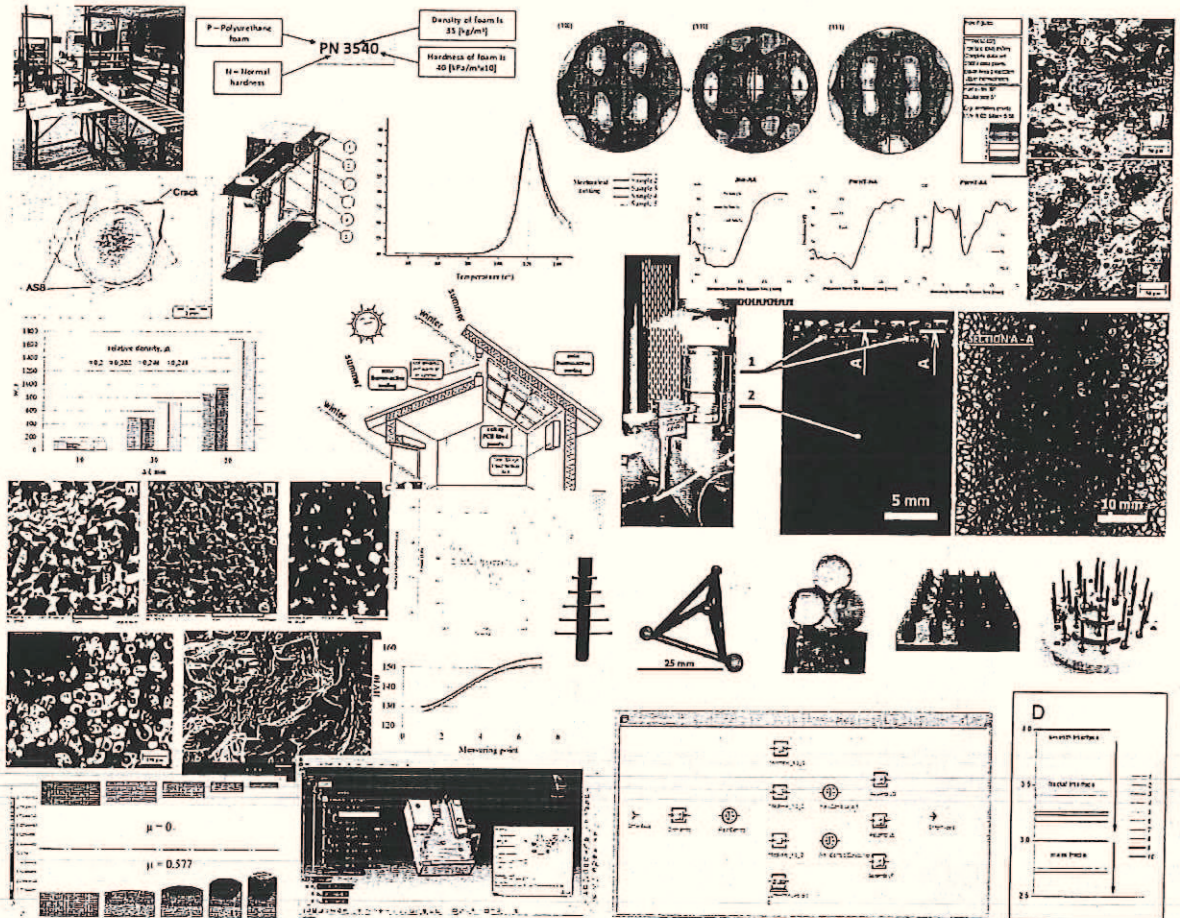
# 9<sup>th</sup> International Conference

ISSN 1847-7917

## Mechanical Technologies and Structural Materials 2019

General sponsors:

University of Split - FESB,  
The Split - Dalmatia County,  
The City of Split,  
EVN Croatia Plin d.o.o.



<http://www.strojarska-tehnologija.hr>

September, 26<sup>th</sup> - 27<sup>th</sup>, 2019.  
FESB, Ruđera Boškovića 32, Split

# CONFERENCE PROCEEDINGS

## MECHANICAL TECHNOLOGIES AND STRUCTURAL MATERIALS

Split

Croatia

26 - 27 September 2019

### ORGANIZED BY:

CROATIAN SOCIETY FOR MECHANICAL TECHNOLOGIES, Croatia

### CO-ORGANIZERS:

UNIVERSITY OF SPLIT  
FACULTY OF ELECTRICAL ENGINEERING, MECHANICAL ENGINEERING  
AND NAVAL ARCHITECTURE

CROATIAN SOCIETY FOR MATERIALS AND TRIBOLOGY

DUBLIN INSTITUTE OF TECHNOLOGY

SLOVAK ACADEMY OF SCIENCE INSTITUTE OF MATERIALS AND MACHINE  
MECHANICS

ROGANTE ENGINEERING OFFICE

UNIVERSITY OF SPLIT  
UNIVERSITY DEPARTMENT OF PROFESSIONAL STUDIES

**SPONSORS:**

UNIVERSITY OF SPLIT

SPLIT – DALMATIA COUNTY

CITY OF SPLIT

EVN CROATIA PLIN d.o.o. 🍀

TOURIST BOARD OF SPLIT

**PUBLISHER:**

CROATIAN SOCIETY FOR MECHANICAL TECHNOLOGIES, Croatia

HRVATSKO DRUŠTVO ZA STROJARSKE TEHNOLOGIJE, Hrvatska

c/o FESB, Ruđera Boškovića 32, 21000 SPLIT

tel.: +385 21 305 910; fax.: +385 21 463 877

e-mail: [info@strojarska-tehnologija.hr](mailto:info@strojarska-tehnologija.hr)

<http://www.strojarska-tehnologija.hr>

**EDITORS:**

PhD Sonja Jozić, Associate Professor

PhD Branimir Lela, Associate Professor

ISSN 1847-7917

ISSUE: 70

## ORGANIZING COMMITTEE:

- Sonja JOZIĆ (Croatia) - Chairman
- Branimir LELA (Croatia) – Vice Chairman
- Ante ALUJEVIĆ (Croatia)
- Andrej Bašić (Croatia)
- Nikša ČATIPOVIĆ (Croatia)
- Zvonimir DADIĆ (Croatia) #
- Ivana DUMANIĆ (Croatia)
- Igor GABRIĆ (Croatia)
- Nikola GJELDUM (Croatia)
- Dario ILJKIĆ (Croatia)
- Jure KROLO (Croatia)
- Petar LJUMOVIĆ (Croatia)
- Zvonimir MRDULJAŠ (Croatia)
- Stipe PERIŠIĆ (Croatia)
- Slaven ŠITIĆ (Croatia)

## PROGRAMME AND REVIEW COMMITTEE:

- Dražen ŽIVKOVIĆ (Croatia) – President
- Dražen BAJIĆ (Croatia) – Vice President
- Boris ANZULOVIĆ (Croatia)
- Frane BARBIR (Croatia)
- Franjo CAJNER (Croatia)
- Goran CUKOR (Croatia)
- Krešimir GRILEC (Croatia)
- Vinko IVUŠIĆ (Croatia)
- Zlatko JANKOSKI (Croatia)
- Jaroslav JERZ (Slovakia)
- Sonja JOZIĆ (Croatia)
- David KENNEDY (Ireland)
- Branimir LELA (Croatia)
- Zoran PANDILOV (Macedonia)
- Mladen PERINIĆ (Croatia)
- Massimo ROGANTE (Italy)
- Zdravko SCHAUPERL (Croatia)
- František SIMANČIK (Bratislava)
- Božo SMOLJAN (Croatia)
- Goran ŠIMUNOVIĆ (Croatia)
- Katica ŠIMUNOVIĆ (Croatia)
- Matej VESENJAK (Slovenia)
- Ivica VEŽA (Croatia)



*Mechanical Technologies  
and Structural Materials  
MTSM2019*

# Different corrosion behaviour of CuNi10Fe1Mn alloy condenser tubes in seawater

Zvonimir DADIĆ<sup>1)</sup>, Senka GUDIĆ<sup>2)</sup>,  
Ladislav VRŠALOVIĆ<sup>2)</sup>, Dario  
KVRGIĆ<sup>2)</sup>, Ivana IVANIĆ<sup>3)</sup>, Nikša  
ČATIPOVIĆ<sup>1)</sup>

- 1) University of Split, Faculty of Electrical Engineering, Mechanical Engineering and Naval Architecture, Ruđera Boškovića 32, 21000 Split, Croatia
- 2) University of Split, Faculty of Chemistry and Technology, Ruđera Boškovića 35, 21000 Split, Croatia
- 3) University of Zagreb, Faculty of Metallurgy, Aleja narodnih heroja 3, 44103 Sisak, Croatia

[zdadic@fesb.hr](mailto:zdadic@fesb.hr)

## Keywords

*CuNi10Fe1Mn alloy*

*Corrosion*

*Microstructure*

*Polarization*

*SEM/EDS analysis*

## 1. Introduction

Copper-based alloys have a long history of marine environment service because of their attractive combination of properties, e.g., good machinability, good resistance to corrosion and biofouling, and superior thermal and electrical conductivity [1-4]. Among those, Cu-Ni alloys are used for condenser tubing in marine applications where good resistance to localized corrosion (pitting) and erosion corrosion is important. The two most popular alloys contain 90% or 70% copper but the 90-10 copper nickel (CuNi10Fe1Mn) is more economic and extensively used [2]. Prerequisite for good corrosion resistance is the formation of an optimum protective layer on alloy surfaces. Its good corrosion resistance has been attributed to existence of thin, strongly adherent inner Cu<sub>2</sub>O film and porous and thick outer layer. Its composition and thickens strongly depend on the conditions of the media to which the Cu-Ni alloy is exposed to. It also depends on electrolyte composition, temperature, flow velocity etc. [4-9]. The synergistic effect between nickel and iron in CuNiFe alloys with Ni content up to 30 % and iron content up to 2% was established [5,10]. Nickel improves the corrosion resistance of copper by its incorporation into continuous cuprous oxide film and the beneficial effect of iron was

## Professional article

**Abstract:** Two CuNi10Fe1Mn condenser tube samples from boat heat exchangers were investigated due to their different corrosion behaviour in exploitation. One tube was in exploitation nearly 20 years before significant corrosion damage occurred (sample 1), while second tube of different manufacturer showed corrosion damages in 2 months of exploitation (sample 2). In its working conditions seawater was passing through the pipes and R407C gas around the pipes. Chemical analysis, microstructural and hardness investigations and laboratory electrochemical investigations of corrosion behaviour of samples in sea water were performed in order to determine the main reason for different durability of condenser tubes. After electrochemical investigations the polarization surface damage was verified by SEM analysis. Both samples belong to the CuNi10Fe1Mn alloy system with the significant difference in the mass fraction of iron content (around 30% higher for sample 1). Samples coincide in the structural sense (type and size of grain) and in mechanical properties (hardness of 133 HV<sub>1</sub>). Fe content in the CuNi10Fe1Mn alloy has the key role in the corrosion behaviour of the tested samples. It has been found that (regardless of the temperature of the heat exchanger) the corrosion resistance of the tested samples increases with increasing Fe content in the alloy. Namely, the corrosion current decreases in same order, while the polarization resistance and properties of surface oxide layer increase. SEM analysis confirmed less damage on the surface of samples with higher Fe content.

explained by the formation of  $\gamma$ -FeO (OH) [10,11]. Erosion in combination with pollution is the major reason for corrosion failure of CuNi10Fe1Mn alloys exposed to seawater [6,8]. In polluted water containing hydrogen sulphide the corrosion potential is shifted to the negative values and pitting corrosion evolves usually in the form of wide and shallow pits [8]. Care should be taken if there is a risk of prolonged exposure to sulphide polluted water as is commonly the case in harbours and brackish water. Under-deposit corrosion can be evolved if the region under deposits becomes anaerobic due to the establishment of sulphate reducing bacteria. Then the situation can become critical [8]. When the flow velocity of seawater becomes too large, local turbulence may occur, which can damage the protective film. Then the corrosion at isolated spots can start due to galvanic action between the base metal underneath the damaged film and the film itself [7]. This galvanic effect may be worsened by the unfavourable ratio of the area of the base metal to the much larger film area.

The aim of the present investigation is to determine the reason for different corrosive behaviour of two CuNiFe1Mn condenser tubes (delivered from different manufacturers) that were incorporated into the ship's cooling system.

## 2. Experimental work

Two different CuNi10Fe1Mn condenser tube samples from boat heat exchangers were investigated. One tube was in exploitation nearly 20 years (sample 1), while second tube of different manufacturer was in exploitation for 2 months (sample 2). In its exploitation seawater was passing through the pipes and R407C gas around the pipes. Both samples were subjected to extensive testing. Tests include the determination of chemical composition, structural analysis, hardness test and corrosion behaviour in seawater. Figure 1 shows the CuNi10Fe1Mn tube samples that were taken for this investigation.

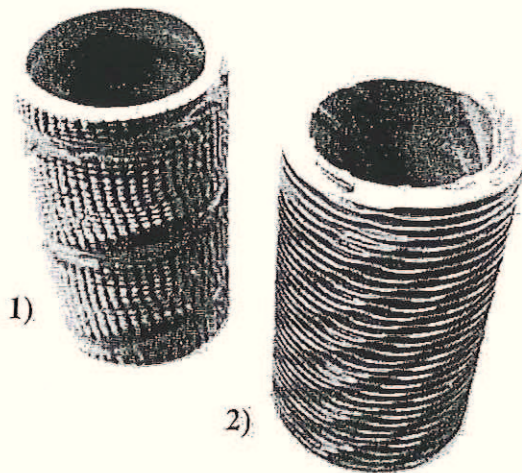


Figure 1. CuNi10Fe1Mn alloy tube samples 1 and 2

Chemical analysis of the investigated alloy samples 1 and 2 was made with Olympus DS2000-C XRF using a non-destructive test method according to norm ASTM E1621-94.

For the microstructural analysis tube samples were cut in small pieces wherein the samples were cooled with a cooling agent. After cutting, sample surfaces were prepared by grinding and polishing and thereafter by etching with 50% water solution of nitric acid. Etching time was 30 s. Microstructural analysis was performed on the light microscope OPTON Axioscope.

The hardness of samples 1 and 2 was determined according to EN ISO 6507-1: 2018 standard by Vickers method using Shimadzu HMV-2T microhardness tester. On each sample, the measurement was repeated 5 times with the testing force of 9.807 N (HV1).

Corrosion behaviour of tested samples was examined in naturally aerated sea water (pH=8.2) at temperature of 20 °C and 40 °C, which was also the working temperature range of the heat exchanger in exploitation. For this purpose, the working electrodes were made by cutting CuNi10Fe1Mn condenser tubes into small square samples and then soldering one side of samples with isolated copper wire to gain good electrical contact. After

soldering, sample surfaces were isolated with epoxy resin leaving one side of the surface to be in contact with the electrolyte. The measurements were performed in conventional three-electrode double wall glass electrochemical cell, with a platinum counter-electrode and a saturated calomel reference electrode, respectively. Before each experiment, the working electrode was polished mechanically using successive grades of emery paper up to 1200 grit. The electrode was then ultrasonically washed with ethanol, rinsed with deionized water and transferred quickly to the electrochemical cell filled with electrolyte (i.e. sea water).

Electrochemical measurements were carried out with the PAR 273A potentiostat/galvanostat. Open circuit potential measurements ( $E_{oc}$ ) were carried out immediately after electrode immersion in electrolyte in 60 minutes period. Linear polarization measurements were carried out in the potential range of  $\pm 20$  mV around  $E_{oc}$  with the scan range of 0.2 mV/s. Potentiodynamic polarization measurements were performed in the potential range of  $\pm 250$  mV from  $E_{oc}$  with the scan rate of 0.2 mV/s.

After polarization measurements the electrode surfaces were cleaned ultrasonically with deionized water and then examined with scanning electron microscope (SEM) Tescan Vega TS5136LS.

## 3. Results and discussion

At the beginning of the examination chemical analyses were performed in order to detect possible differences in the chemical composition of the tested alloy. The results of the investigations are given in Table 1 along with the data for the standard alloy classification according to the EN 12449:2016-11.

From the Table 1 it is evident that both samples belong to the CuNi10Fe1Mn alloy system with significant difference in the mass fraction of iron content (around 30% higher for sample 1).

The results of the microstructural analysis are given in Figure 2.

Microstructures of tested samples correspond to microstructure of CuNi10Fe1Mn alloy, which consists of copper-based crystals (FCC) [12].

Isolated dark areas are the result of segregation of alloying elements [13]. Also, it is shown in Figure 2 that sample 2 has more segregated alloying elements.

Hardness testing results can be seen in Figure 3. It was found that both samples have the same hardness, 133 HV<sub>1</sub>, which implies that they have similar mechanical properties.

In order to better determine the reasons for the different durability (corrosion) of two CuNiFe1Mn condenser tubes that were incorporated into the ship's cooling system, its real working conditions were simulated.



Table 1. Results of the chemical analysis of samples

Sample	%					
	Mn	Fe	Ni	P	S	Cu
1	0.82	1.92	9.55	0.017	0.016	balance
2	0.82	1.36	9.56	0.009	0.028	balance
<i>Chemical composition of CuNi10Fe1Mn according to the EN 12449:2016-11</i>						
EN min.	0.5	1	9	0	0	balance
EN max.	1	2	11	0.02	0.05	balance

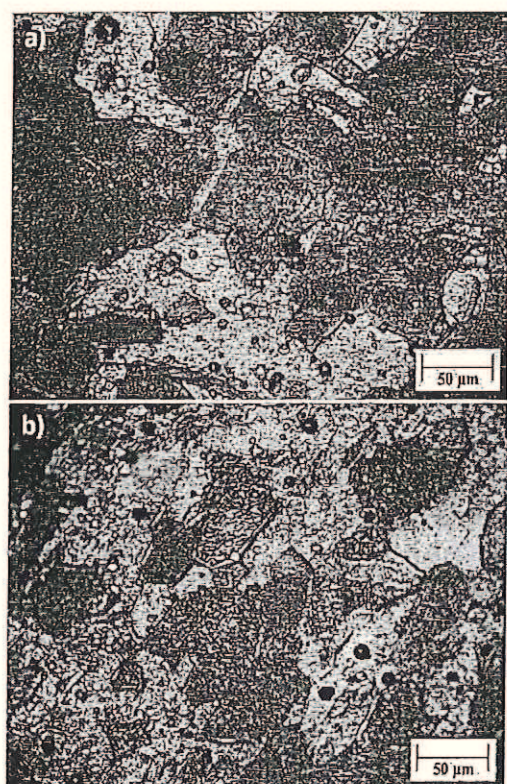


Figure 2. Microstructural analysis of samples 1 (a) and 2 (b)

Namely, the corrosion behaviour of tested samples was examined in naturally aerated sea water (pH = 8.2) at the temperature of 20 °C and 40 °C, which is also the working temperature range of the heat exchanger in exploitation. Figure 4 shows the variation of  $E_{OC}$  of tested samples with time in sea water at 20 °C.

The open circuit potential reflects the composite results of the electrochemical reactions which take place at the electrode/solution interface. As can be seen, both samples show similar changes of  $E_{OC}$ . Namely, immediately after immersing each electrode in sea water, values of  $E_{OC}$  were shifted towards negative values due to the adsorption of chloride ions on the surface of the electrode [14,15].

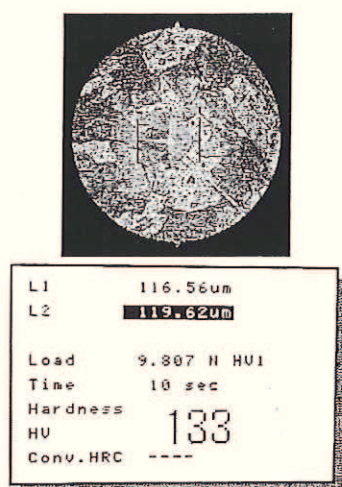


Figure 3. Vickers hardness indentation test

After the initial drop,  $E_{OC}$  of both electrodes increased towards positive values which indicated the formation and thickening of the protective passive film on their surfaces during the immersion. The stabilization of  $E_{OC}$  for both samples occurs in period of 20 minutes. It can also be noted that the sample 2 has more negative  $E_{OC}$  value. The general corrosion behavior of tested samples in sea water was investigated by recording the polarization curves in wide potential range.

The purpose of these measurements was to evaluate influence of different Fe content on anodic and cathodic behavior of CuNi10Fe1Mn alloy and determination of corrosion current density ( $i_{corr}$ ) and corrosion potential ( $E_{corr}$ ). Obtained results are presented on Figure 5 and Table 2. Significant differences in corrosion behaviour of samples 1 and 2 can be noticed.

The gradual reduction of the anodic and cathodic current density and shift of corrosion potential value in the anodic side can be observed with increasing Fe content in the alloy.

This direction of change ultimately leads to a reduction in the corrosion rate. As can be seen from Table 2 the significantly lower  $i_{corr}$  and the most positive  $E_{corr}$  have been obtained for sample 1 (alloy with the higher Fe

content) which also has the higher polarization resistance,  $R_p$  (i.e. resistance of metal to corrosion).

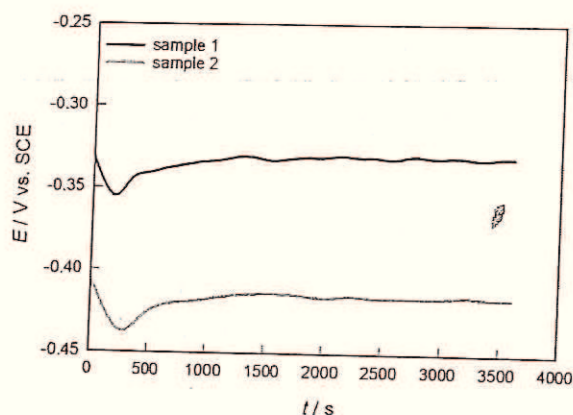


Figure 4. Variation of the open circuit potential of CuNi10Fe1Mn samples in sea water at 20 °C

The  $R_p$  data was determined from the slope of linear part of polarization curves obtained by measurements in the potential range close to  $E_{oc}$  (Figure 6). Thus, it can be concluded that the content of Fe has a key role in corrosion behaviour of CuNi10Fe1Mn alloy.

In order to better simulate the real conditions of the heat exchanger, the polarization measurements were carried out in sea water at 40 °C, and obtained results are also presented in Table 2. By increasing the temperature, the corrosion resistance of sample with a smaller Fe content (sample 2) is significantly reduced (higher  $i_{corr}$ , lower  $R_p$ ).

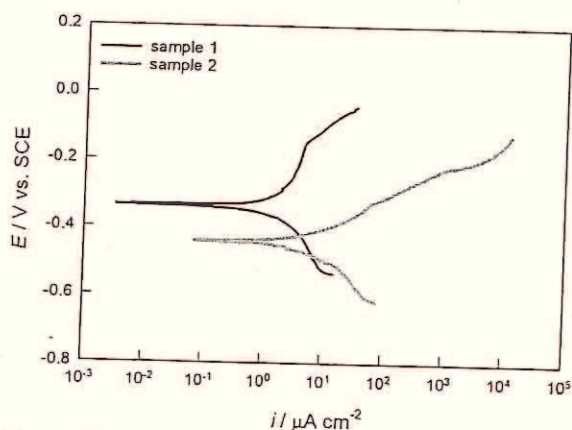


Figure 5. Variation of the open circuit potential of CuNi10Fe1Mn samples in sea water at 20 °C

However, it is interesting that the corrosion resistance of the sample with a higher Fe content (sample 1) remains unchanged, indeed even increases slightly. Similar behaviour of CuNiFe alloys were observed in literature and can be related with beneficial influence of temperature on protective properties of surface oxide layer [8].

Table 2. Corrosion parameters of investigated CuAlMn alloys in 0.9% NaCl solution

sample	$E_{corr}$ / V	$i_{corr}$ / $\mu\text{A cm}^{-2}$	$R_p$ / $\text{k}\Omega \text{ cm}^{-2}$
20 °C			
1	-0.33	2.16	14.60
2	-0.45	7.94	3.04
40 °C			
1	-0.35	2.04	14.75
2	-0.47	17.15	0.93

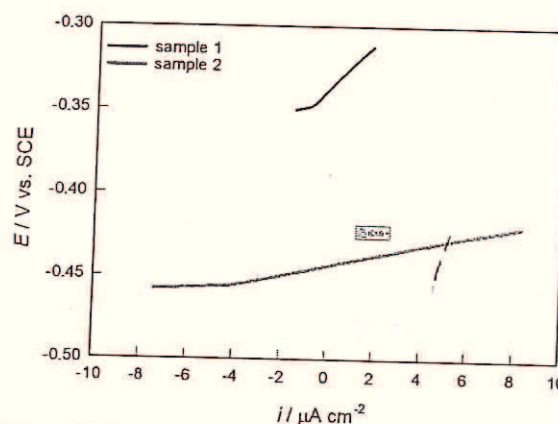


Figure 6. Linear parts of polarization curves of CuNi10Fe1Mn samples in sea water at 20 °C

After electrochemical investigations the polarization surface damages were verified by SEM, and obtained results are shown on Figures 7 and 8. The rough surface defects resulting from significant corrosion are visible on the surface of samples 2 (Figure 7b), while the surface of sample 1 is almost clear of any corrosion damage; only one shallow pit is visible (Figure 7a). Surface damage of both samples is higher at 40 °C (Figure 8).

According to the EN 12449:2016-11, the content of Fe in CuNi10Fe1Mn of the alloy may vary within the range of 1 to 2% (Table 1). Although the change of Fe content in these boundaries does not affect the structural (Figure 1) and mechanical properties (Figure 2) it is obvious that it significantly affects the corrosion behaviour of CuNi10Fe1Mn alloys (Figures 3-5, Table 2) which was additionally confirmed by SEM surface analysis (Figures 7 and 8).

Corrosion resistance is the consequence of the formation of a surface layer whose properties primarily depend on the chemical composition of the base metal. The type and content of the particular alloying elements in the sample (Table 1).

If the alloying element facilitates the passivity of copper, the surface film properties will be better (greater resistance and thickness, more compact structure).

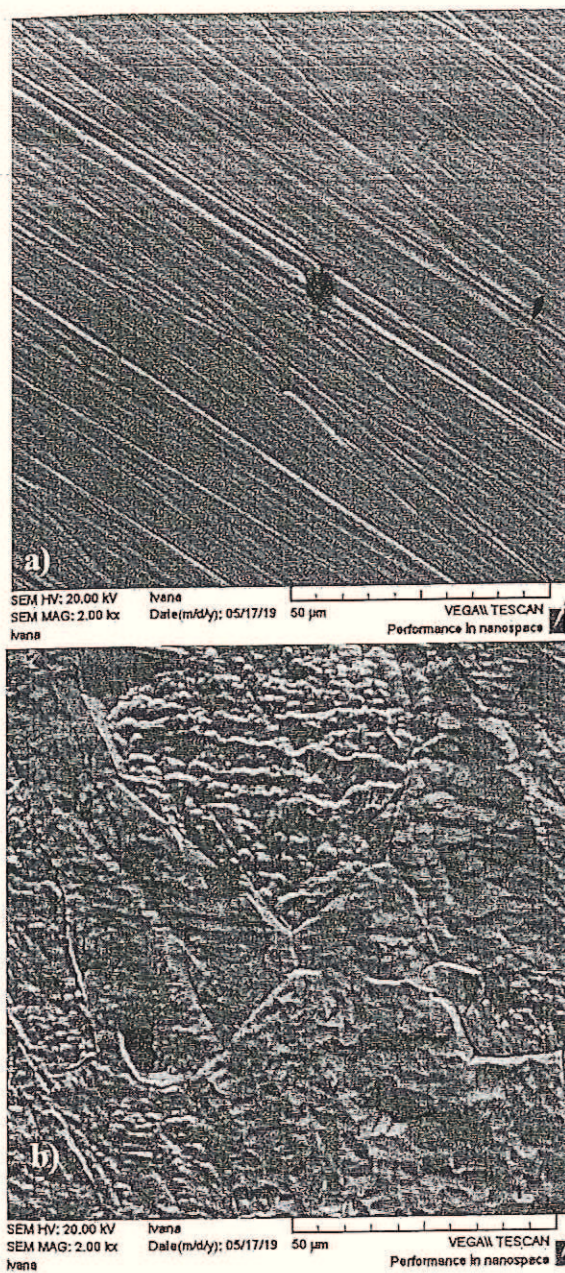


Figure 7 SEM images of the electrode surfaces after potentiodynamic polarization measurements at 20 °C for sample 1 (a) and sample 2 (b)

Such impact of the alloyed element will ultimately lead to higher corrosion resistance of the metal in the aggressive media, smaller corrosion currents and greater polarization resistance. According to obtained data, it can be concluded that the content of Fe has a key role in passivation of CuNi10Fe1Mn alloy.

As previously mentioned, good corrosion resistance of CuNiFe alloys has been attributed to existence of thin, strongly adherent inner  $\text{Cu}_2\text{O}$  film and porous and thick outer layer [4-9].

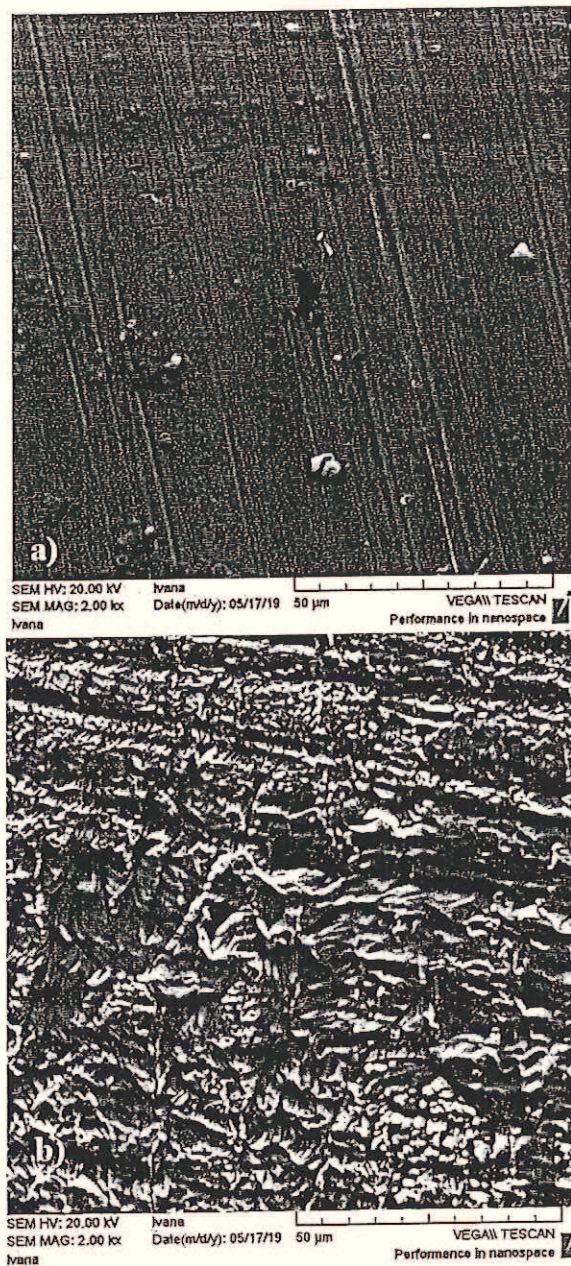


Figure 8. SEM images of the electrode surfaces after potentiodynamic polarization measurements at 20 °C for sample 1 (a) and sample 2 (b)

The synergistic effect between nickel and iron in CuNiFe alloys with Ni content up to 30 % and iron content up to 2% were established [5,10]. Nickel improves the corrosion resistance of copper by its incorporation into continuous cuprous oxide film and the beneficial effect of iron was explained by the formation of  $\gamma\text{-FeO(OH)}$  [10,11].

The role of alloying elements (in this case Fe) on metal passivation can be explained by the model proposed by

Marcus [16]. The model is based on two fundamental properties of metals, such as:

- strength of the oxygen (or OH) chemisorption bond,  $\varepsilon_{M-O}$ , (reflected by the value of the heat of oxygen adsorption,  $\Delta H_{ads(Ox)}$ );
- the facility of conversion from the oxygen (or OH) monolayer to a 3D oxide in which a critical factor is disruption of the metal-metal bonds (reflected by metal-metal bond energy,  $\varepsilon_{M-M}$ ) [16].

Passivation usually begins by adsorption of oxygen or OH from the water solution, followed by nucleation and oxide growth. Obviously, metals with high heat of oxygen adsorption are easily passivated. However, it is less apparent and less recognizable that the passive film formation requires additional activation energy for conversion of chemisorbed layer into 3D oxide, and that this process inevitably leads to a metal-metal interruption. Therefore, the lower the energy required to disrupt metal-metal bonds, the lower the activation energy barrier for the conversion into 3D oxide [16]. The metals which adsorb oxygen (or OH) strongly and on which metal-metal bonds are easily broken will be very suitable for the passive oxide film growth. Hence, alloying elements with high energy adsorption of oxygen, and low metal-metal bonds energy, reinforce the passivation of the base metal. However, the easy metal-metal bond disruption will also accelerate metal dissolution. Therefore, fine balancing between the effect of metal-metal bonding energy and the effect of oxygen adsorption heat is crucial in design of alloys which can passivate.

Based on such considerations, it is possible to divide alloying elements on passivity promoters and dissolution moderators or blockers. According to Marcus [16], metals with high  $\Delta H_{ads(Ox)}$  and a relatively low  $\varepsilon_{M-M}$  like Cr, Al, Ti belong to passivity promoters, i.e. the alloying elements that facilitate passivation of the metal.

By the amount of heat oxygen adsorption and bond energy Fe is very similar to Cr. A large amount of energy released during the adsorption of oxygen is able to easily disrupt Fe-Fe bonds, thus causing oxide nucleation much before completion of the adsorbed monolayer. Therefore, when the Fe content of the alloy is higher (sample 1), it is easier to form a 3D compact oxide layer consisting of a mixture of oxides Cu, Ni i Fe [5,10,11]. 3D surface layer efficiently separates metal from the aggressive medium and prevents corrosion of the alloy. Working conditions of marine heat exchangers lead to increase in seawater temperature, which further improves the protective properties of the oxide layer [8].

#### 4. Conclusion

Both samples belong to the CuNi10Fe1Mn alloy system with the significant difference in the mass fraction of iron content (around 30% higher for sample 1). Samples

coincide in the structural sense (type and size of grain) and in mechanical properties.

Fe content has the key role in the corrosion behavior of the tested samples in CuNi10Fe1Mn alloy. It has been found that (regardless of the temperature of the heat exchanger) the corrosion resistance of the tested samples increases with increasing Fe content in the alloy. Namely, the corrosion current decreases in same order, while the polarization resistance and properties of surface oxide layer increase. SEM analysis confirmed less damage on the surface of samples with higher Fe content.

#### REFERENCES

- [1] Ateya B.G., Ashour E.A., Sayed M.S., (1994), *Corrosion of  $\alpha$ -Al bronze in saline water*, J. Electrochem. Soc. 141, p 71-78, Germany
- [2] Powell C., *Corrosion and Biofouling Resistance Evaluation of 90-10 Copper-Nickel*, <https://docplayer.net/21504306-Corrosion-and-biofouling-resistance-evaluation-of-90-10-copper-nickel.html> (27. 5. 2019.)
- [3] Davis J.R., (2001), *Alloying: Understanding the basics*, ASM International, USA
- [4] Aljinović Lj., Gudić S., Šmith M., (2000), *Inhibition of CuNi10Fe corrosion in seawater by sodium-diethyl-dithiocarbamate: an electrochemical and analytical study*, J. Appl. Electrochem. 30, p 973-979, Netherlands
- [5] Badawy W.A., Ismail K.M., Fathi A.M., (2005) *Effect of Ni content on the corrosion behavior of Cu-Ni alloys in neutral chloride solutions*, Electrochim. Acta 50, p 3603-3608, UK
- [6] Kievits F.J., Ijsseling F.P., (1972), *Research into the corrosion behaviour of CuNi10Fe alloys in seawater*, Werkstoffe und corrosion 12, p 1084-1096, Germany
- [7] Ijsseling F.P., (1974), *The application of the polarization resistance method to the study of the corrosion behaviour of CuNi10Fe in sea-water*, Corros. Sci. 14, p 97-110, England
- [8] Schleich W., *Application of copper -nickel alloy UNS C70600 for seawater service*, URL: [https://www.copper.org/applications/marine/cuni/alloys/uns\\_c70600.html](https://www.copper.org/applications/marine/cuni/alloys/uns_c70600.html) (10. 7. 2019.)
- [9] Hack H.P., Pickering H.W. (1991), *AC impedance study of Cu and Cu-Ni alloys in aerated saltwater*, J. Electrochem. Soc. 138, p 690-695, USA
- [10] Milošev I., Metikoš-Huković M. (1997), *The behaviour of Cu-xNi (x = 10 to 40 wt%) alloys in alkaline solutions containing chloride ions*, Electrochim. Acta, 42, p 1537-1548, UK
- [11] Milošev I., Metikoš-Huković M. (1999), *Effect of chloride concentration range on the corrosion resistance of Cu-xNi alloys*, J. Appl. Electrochem. 29, p 393-402, Netherlands

- [12] Brandes E. A.: Smithells Metals Reference Book, Seventh Edition, Butterworth & Co., 1983.
- [13] Kievits, F. J., & Ijsseling, F. P. (1972), Research into the corrosion behaviour of CuNi10Fe alloys in seawater. Materials and Corrosion/Werkstoffe Und Korrosion, 23(12), 1084–1096, Germany
- [14] Vrsalović L., Oguzie E., Kliškić M., Gudić S. (2011), Corrosion inhibition of CuNi10Fe alloy with phenolic acids, Chem. Eng. Comm. 198, p 1380-1393, UK
- [15] Alfantazi A.M., Ahmed T.M., Tromans D. (2009), Corrosion behaviour of copper alloys in chloride media, Mater. Design 30, p 2425–2430, Netherlands
- [16] Marcus P. (1994), On some fundamental factors in the effect of alloying elements on passivation of alloys, Coros. Sci. 36, p 2155-2158,